Optics Letters

Millijoule-level, kilohertz-rate, CPA-free linear amplifier for 2 μm ultrashort laser pulses

Moritz Hinkelmann,[1,*] Bastian Schulz,[2] Dieter Wandt,[1] Uwe Morgner,[1,3] Maik Frede,[2] Jörg Neumann,[1] and Dietmar Kracht[1]

[1]Laser Zentrum Hannover e.V., Laser Development Department, Ultrafast Photonics Group, Hollerithallee 8, D-30419 Hannover, Germany
[2]neoLASE GmbH, Hollerithallee 17, D-30167 Hannover, Germany
[3]Institut für Quantenoptik, Leibniz Universität Hannover, Welfengarten 1, D-30167 Hannover, Germany
*Corresponding author: m.hinkelmann@lzh.de

Received 2 October 2018; revised 1 November 2018; accepted 7 November 2018; posted 7 November 2018 (Doc. ID 346692); published 29 November 2018

The generation of millijoule-level ultrashort laser pulses at a wavelength of 2.05 μm in a compact chirped pulse amplification-free linear amplifier based on Holmium-doped YLF gain medium is presented. More than 100 MW of pulse peak power has been achieved. We show the capabilities of this laser amplifier from a 1 kHz to 100 kHz repetition rate. A detailed numerical description supports the experimental work and verifies the achieved results.

https://doi.org/10.1364/OL.43.005857

In the past years, high-energy ultrashort pulse laser development in the wavelength region around 2 μm has been promoted by a strong application-driven demand. This includes the generation of mid-infrared (mid-IR) radiation in nonlinear optical parametric conversion stages [1,2], as well as applications in medicine, communication, micromachining of polymers, and metrology [3]. However, pulses with a broad spectrum below 2 μm experience detrimental atmospheric water absorption which leads to a pulse shape degradation in the time domain and distortions of the transverse beam profile in the spatial domain [4]. One approach to prevent such effects is using in-band pumped Holmium (Ho)-doped crystals with emissions beyond 2 μm out of the strong water absorption lines. Ho-doped crystals benefit from their advantageous properties such as high gain, low quantum defect, broad spectral bandwidth to support ultrashort pulse duration, and a long upper laser level lifetime [3]. Commonly, high-energy laser pulses with pulse durations below 10 ps are generated via chirped pulse amplification (CPA).

The most widely used gain materials are Ho-doped $Y_3Al_5O_{12}$ (YAG) and $YLiF_4$ (YLF). Next to the superior mechanical properties of the Ho:YAG crystal, Ho:YLF benefits from a longer upper laser level lifetime, a significantly lower nonlinear refractive index, and a low negative thermal coefficient of the refractive index $\mathrm{d}n/\mathrm{d}T$ [5]. In addition, Ho:YLF is an intrinsically birefringent material. This is beneficial at high pump power levels for the reduction of depolarization losses due to thermally induced birefringence. In fact, several multi-millijoule CPA laser systems have been reported which unite high pulse energies and, after proper compression, ultrashort sub-10 ps pulse durations, resulting in a pulse peak power suitable for the aforementioned mid-IR generation [2,6–9]. However, the achievable output pulse energy depends on bulky, expensive pulse stretchers and compressors, and their efficiencies. As a consequence, these systems consist of complex, table-top-size setups.

Pushing the pulse repetition frequency (PRF) towards tens of kilohertz (kHz) is interesting, especially, for applications in micromachining as well as in medicine. In addition, maintaining megawatt- (MW) level ultrashort pulses is challenging. Commonly, a Pockels cell is used as optical switch in CPA-based regenerative amplifiers. However, a high pick rate in combination with high voltage leads to adverse effects resulting in piezoelectric ringing or resonance effects [10]. In addition, the Pockels cell consists of one or multiple crystals which are not capable of handling MW-level pulse peak power due to the large amount of accumulated nonlinear phase. This results in a restriction of Pockels cell-based ultrashort pulse amplifiers to the CPA scheme only. Just recently, we reported on multipass amplification of ultrashort pulses in a simplified CPA-free approach based on highly doped Ho:YLF crystals [11]. This laser system was capable of generating MW-level pulse peak powers covering PRFs ranging from 10 to 500 kHz.

In this contribution, we show further energy scaling and, to the best of our knowledge, first CPA-free amplification of ultrashort pulses to millijoule- (mJ) level in Ho:YLF crystals. The setup is based on a linear amplification scheme with highly doped gain crystals. At the same time, the entire laser system fits on a small 1 m^2 breadboard area. Numerical simulations have been used to preselect a setup with appropriate parameters. We will compare the simulated and the experimental results and show scaling options.

The layout of the laser system, as depicted in Fig. 1, consists of an all-fiber ultrashort pulse seeder, an acousto-optical modulator (AOM) to pick the pulses, a multipass high gain

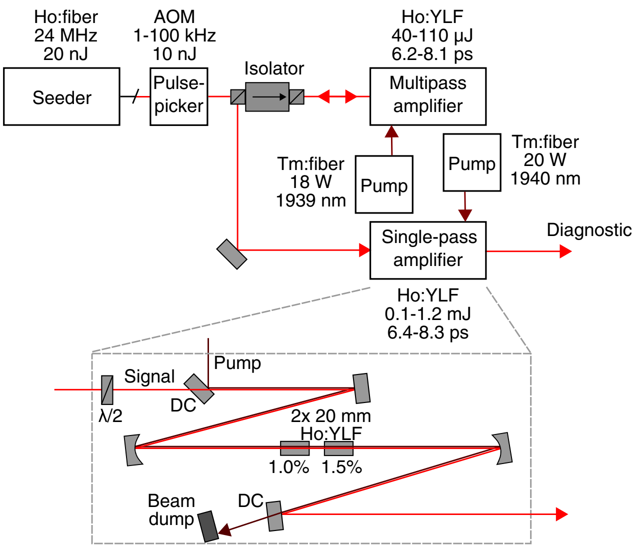

Fig. 1. Schematic setup of the amplifier. AOM, acousto-optic modulator; $\lambda/2$, half-wave plate; DC, dichroic mirror.

linear amplifier, and a single-pass booster stage. The seed source provides 5-ps pulses at a wavelength of 2.05 µm and has been similarly published in [12]. A free-space AOM reduces the PRF from MHz-level to kilohertz. The following multipass amplification stage based on Ho(1.5 at. %):YLF has been published in [11] and generates up to about 100-µJ pulses with a pulse duration of 8 ps at a repetition rate of 1 kHz. A final single-pass amplifier boosts the pulse energy up to the mJ-level, maintaining ultrashort pulse duration. The whole amplifier chain is CPA-free; thus, no stretcher or compressor is required.

Different a-cut Ho-doped YLF crystals with lengths of 20 mm and doping concentrations between 0.5 and 1.5 at. % have been available for the presented experiments. In order to investigate the lifetime quenching, which may emerge in Ho-doped materials at dopant concentrations above 0.5 at. %, we measured the excited state fluorescence lifetime of the transition $^5I_7 \rightarrow {}^5I_8$. The results are summarized in Fig. 2. At the lowest doping concentration of 0.5 %, the lifetime is almost independent of the pump intensity and in line with the literature

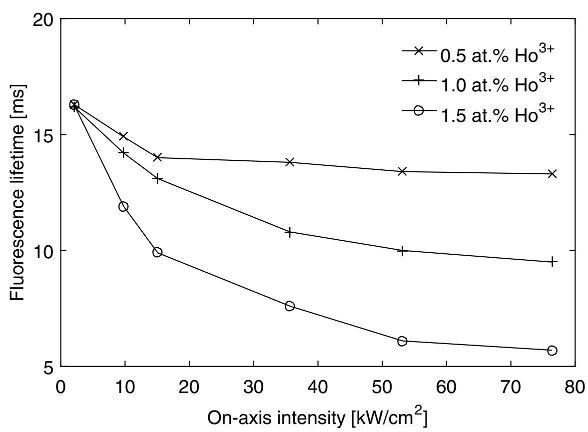

Fig. 2. Measured excited state fluorescence lifetime of Ho-doped YLF crystals with doping concentrations between 0.5 and 1.5 at. %, depending on the excitation intensity.

values of about 14 ms [13]. In contrast, higher doping concentrations show a decrease of the lifetime in dependence on the excitation intensity, resulting in a lifetime of about 10 and 6 ms for doping concentrations of 1.0 and 1.5 %, respectively.

The high pulse peak intensities in the CPA-free single-pass booster stage require a careful study of the intensity evolution within the amplifier medium. On one hand, small beam diameters are beneficial for proper amplification, whereas the high intensities in the focal area potentially damage the gain medium. Preliminary simulations can provide a set of reasonable setup parameters such as doping concentration, crystal length, and focal beam size. Recent publications on the numerical simulation of the energy built up in regenerative amplifiers are commonly based on a modified Frantz-Nodvik formalism. These are able to compute spectral effects such as gain narrowing or re-absorption of quasi-three-level gain media, as in the case of Ho:YLF. In Ref. [14], the pump and amplification phases are calculated sequentially. The inverted fraction is iterated along the propagation axis of the gain medium with a fixed pump and laser mode diameter. A similar approach has been presented by Kroetz *et al.* [15], where the inverted fraction is updated after each pump and amplification cycle, however, without slicing the gain medium along the propagation direction. Here we use an approach similar to the one described in Ref. [15], but with sequential calculation of the pulse evolution by longitudinal splitting of the gain medium in vertical slices and, at the same time, adapting the beam size for every crystal slice. In this way, we are able to determine the pulse peak intensity for each corresponding crystal slice. For the following numerical analysis of the single-pass booster stage at 1 kHz, the multipass amplifier provides the seed input parameters such as optical spectrum, pulse energy, and pulse duration. We considered the measured fluorescence lifetime for the corresponding dopant concentrations.

For the single-pass amplifier stage, we applied a dual-crystal setup with a Ho-doping concentration of 1.0 and 1.5 at. %. Using the two different doping concentrations allows us to minimize temperature peaks by a more equalized distribution of the heat load. At the same time, the increasing doping concentration in this dual-crystal design compensates for the exponential decay of the pump light distribution. This leads to an improved homogeneity of the absorbed pump power density. The calculated pump absorption in this configuration is about 80% based on our numerical model. We simulated the output pulse energy, the accumulated nonlinear phase (B-integral), and the highest prevalent pulse fluence for different focal beam sizes in the dual-crystal setup at a PRF of 1 kHz. The results are shown in Fig. 3(a). The maximum simulated pulse energy is as high as 2 mJ at a focal radius of 100 µm. On one hand, it is quickly decreasing for an even tighter focus due to the strongly diverging beam for $\omega_0 < 50$ µm and, on the other hand, it is decreasing due to the generally increasing beam at larger beam waists. Both effects lead to less saturation, thus, less energy extraction. The accumulated B-integral is strongly connected to the pulse energy. It is only significant ($> \pi$) at beam waists of about 30 µm $< \omega_0 <$ 150 µm.

The pulse fluence is an important parameter with respect to damage-induced pulse energy limitations. Laser-induced damage in Ho:YLF with ultrashort pulse irradiation has not been studied so far. In previous experiments with Ho:YLF, bulk damage, as well as damage to the coatings, occurred at

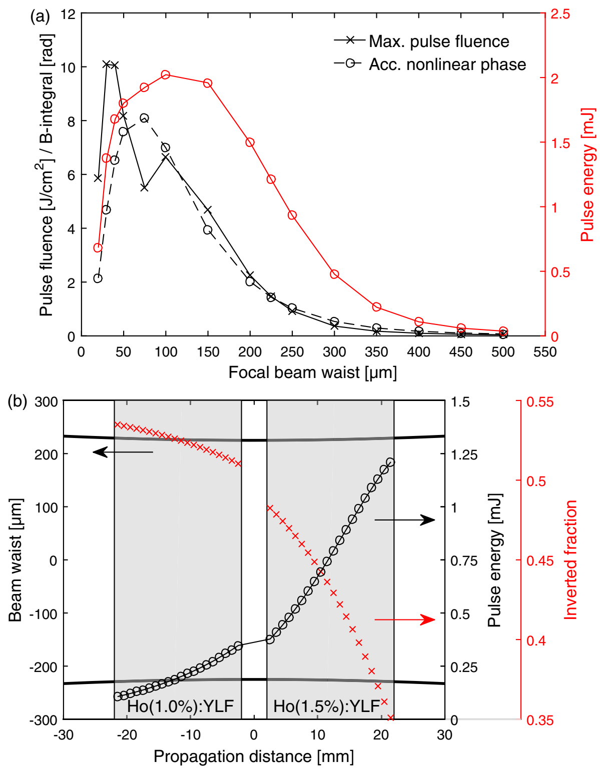

Fig. 3. (a) Simulation results for the dual-crystal single-pass amplifier at a pump power of 20 W and a PRF of 1 kHz. (b) Simulation details with a focal beam radius of 225 μm.

a threshold of about 1.5 J/cm^2 (5 ps). Taking into account the square root scaling law, this leads to a damage threshold of 2 J/cm^2 at a pulse duration of 8 ps. As the square root scaling law might not hold for pulse durations of less than about 10 ps [16], this damage threshold is just a rough estimate. In our simulations, the maximum pulse fluence of 10.1 J/cm^2 is obtained at a focal radius of 30 μm. It is decreasing below 2 J/cm^2 for a beam waist exceeding 200 μm. In order to mitigate damage of the Ho:YLF crystals, we chose a beam waist of 225 μm, corresponding to an operation below 2 J/cm^2 with sufficient prospect of generating mJ-level pulse energies. At the same time, the calculated B-integral, as presented in Fig. 3(a), is only 1.44 rad. Figure 3(b) features a detailed simulation of the dual-crystal amplifier at a focal beam waist of 225 μm with a signal and pump propagation direction from left to right. The shaded area represents the two Ho:YLF crystals and shows the distribution of the inverted fraction (red), which is defined as the ratio of excited ions to the total number of available ions in the gain volume. It is decreasing in propagation direction due to the absorption-induced pump power depletion and stronger saturation of the amplified signal. The two horizontal black lines show the beam caustic with the focus between the two crystals. Finally, the circles show the evolution of the pulse energy. Although the inverted fraction is decreasing from above 50% to about 35% in the second Ho-doped crystal, the gain is significantly stronger due to the higher doping concentration.

In our experiments, both crystals are wrapped in Indium foil and mounted on a water-cooled copper mount. The water temperature was set to 20°C. The pump and signal beams are mode matched and combined by means of a dichroic mirror. A set of two spherical mirrors focuses a pump and signal through the two crystals, starting with Ho(1.0%):YLF followed by Ho (1.5%):YLF. The focal beam waist is calculated to a value of 225 μm located between the two crystals, which are placed about 4 mm apart. Another dichroic mirror separates the unabsorbed amount of pump power and the amplified signal.

The pump source is a customized Tm:fiber-based polarization-maintaining laser amplifier (LISA laser products OHG) which delivers up to 20 W linearly polarized output at a central wavelength of 1940 nm. Pump and signal polarizations are aligned along the c-axis of the uniaxial Ho:YLF gain crystals for the highest efficiency.

The output pulse energies for different PRFs are given in Fig. 4(a). We increased the input seed pulse energy from the front-end multipass amplifier stage and kept the pump power constant at 20 W. The highest pulse energy of 1.2 mJ at 1 kHz corresponds to an average optical power of 1.2 W. The inset of Fig. 4(b) shows the far-field beam profile measured with a scanning slit beam profiler (Ophir NanoScan). The average output power increases to 10.6 W at 100 kHz. The gain factor for the single-pass booster stage is decreasing from 12 at 1 kHz to 2.7 at 100 kHz, as depicted in Fig. 4(b). This can be explained by the increasing average power at higher repetition rates, thus, a decrease of the steady state inversion in the crystal. The measured unabsorbed pump power of about 3.3 W at a PRF of 1 kHz is in the same range as the one simulated with our numerical model. It is worth mentioning that

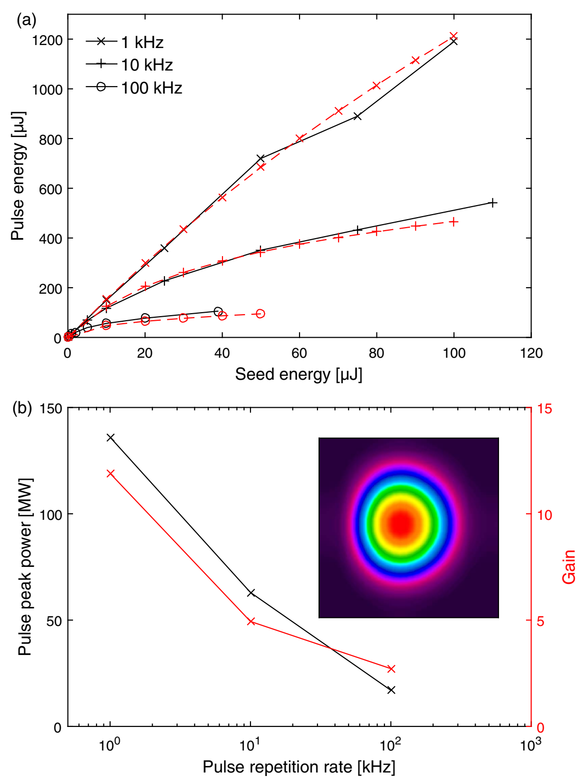

Fig. 4. (a) Numerical (red dashed line) and experimental (black solid line) results showing output pulse energy with increasing seed energy for different PRFs and (b) the corresponding pulse peak powers, as well as the achieved gain factor (inset: far-field beam profile for 1.19 W at 1 kHz).

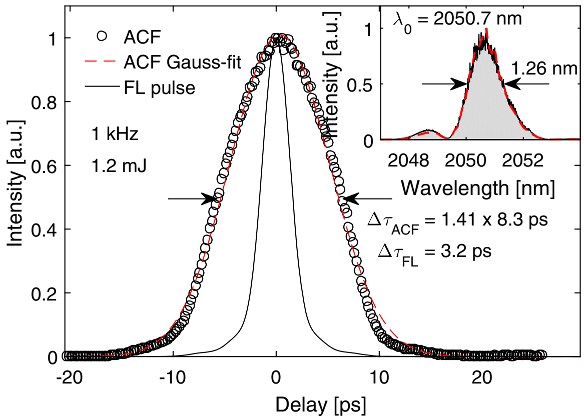

Fig. 5. Autocorrelation trace at a PRF of 1 kHz. The continuous black line is the Fourier-limited pulse duration of the corresponding optical spectrum. Inset: measured (solid black line, shaded area) and simulated (red dashed line) optical spectrum.

during our experiments no laser-induced damage in the Ho:YLF bulk material was observed.

The pulse duration, measured by using an autocorrelator, for a PRF of 1 kHz, is shown in Fig. 5. The pulse duration is 8.3 ps assuming a Gaussian-shaped pulse. The optical spectrum has been measured with an optical spectrum analyzer (YOKOGAWA AQ6375) with a resolution of 0.05 nm. The inset of Fig. 5 shows the corresponding measured (black) and the simulated (red) optical spectrum with a spectral bandwidth of 1.26 nm. The weak peak around 2048.5 nm is a feature of the seed input spectrum. The power spectrum corresponds to a Fourier-limited pulse duration of 3.2 ps. It is worth noting that both the numerical simulations on the output energy in Fig. 4(a), and the optical spectrum in Fig. 5 (inset) is consistent with the experimental results. Considering an input pulse with a duration of 8 ps and a spectral bandwidth of 1.3 nm, the gain narrowing is vanishingly low. We attribute this to the comparably small gain factor in the booster stage. In addition, we did not see any nonlinear effects. This can be explained by the aforementioned low B-integral of 1.44 rad. The measured pulse durations at the PRFs of 10 and 100 kHz are 8.2 and 6.4 ps, respectively. The shorter pulse duration at 100 kHz originates from the shorter seed pulse duration. A summary of the experimental results is given in Table 1.

Considering the achieved sub-10 ps pulse duration and the corresponding pulse energies, we achieved a pulse peak power of 136, 63, and 17 MW at PRFs of 1, 10, and 100 kHz, respectively [Fig. 4(b)]. Nevertheless, the calculated B-integral is in the range of 1.44 rad at the highest achieved pulse energy. This can be attributed to the beneficial low nonlinear refractive index of the YLF host crystal, which is about 1.7×10^{-20} m^2/W [17] compared to 8.1×10^{-20} m^2/W in the case of YAG [18].

Table 1. Summary of the Measured Pulse Energy E_p, Spectral Bandwidth $\Delta\lambda$, and Pulse Duration τ_p for the Amplification in the Dual-Crystal Ho:YLF Amplifier at Different PRFs f_{rep}

f_{rep}	Seed			Amplified		
[kHz]	E_p [μJ]	$\Delta\lambda$ [nm]	τ_p [ps]	E_p [mJ]	$\Delta\lambda$ [nm]	τ_p [ps]
1	100	1.3	8	1.2	1.26	8.3
10	110	1.33	8.1	0.54	1.3	8.2
100	40	1.51	6.2	0.11	1.4	6.4

In conclusion, we have demonstrated a laser system which combines mJ-level pulse energies, a pulse duration below 10 ps, a flexible PRF, and a simplified and compact architecture based on CPA-free amplification. A detailed description of our amplifier by numerical simulations is in line with our experimental results. We believe that further power and energy scaling can be achieved with additional booster stages in order to achieve gigawatt-level pulse peak powers. However, the beam size has to be carefully tailored such that bulk damage in the gain material is mitigated. The investigation of laser-induced bulk damage in Ho:YLF is still pending; thus, potential scaling limitations cannot be foreseen at this point. Nevertheless, the availability of such simplified laser sources will open up a variety of interesting applications.

Funding. Bundesministerium für Bildung und Forschung (BMBF) (13N13974 NUKLEUS).

REFERENCES

1. N. Leindecker, A. Marandi, R. L. Byer, K. L. Vodopyanov, J. Jiang, I. Hartl, M. Fermann, and P. G. Schunemann, Opt. Express **20**, 7046 (2012).
2. M. Hemmer, D. Sánchez, M. Jelínek, V. Smirnova, H. Jelinkova, V. Kubeček, and J. Biegert, Opt. Lett. **40**, 451 (2015).
3. K. Scholle, S. Lamrini, P. Koopmann, and P. Fuhrberg, *Frontiers in Guided Wave Optics and Optoelectronics*, B. Pal, ed. (InTech, 2010) pp. 471–500.
4. M. Gebhardt, C. Gaida, F. Stutzki, S. Hädrich, C. Jauregui, J. Limpert, and A. Tünnermann, Opt. Express **23**, 13776 (2015).
5. R. L. Aggarwal, D. J. Ripin, J. R. Ochoa, and T. Y. Fan, J. Appl. Phys. **98**, 103514 (2005).
6. P. Malevich, G. Andriukaitis, T. Flöry, A. J. Verhoef, A. Fernández, S. Ališauskasa, A. Pugžlys, A. Baltuška, L. H. Tan, C. F. Chua, and P. B. Phua, Opt. Lett. **38**, 2746 (2013).
7. L. von Grafenstein, M. Bock, D. Ueberschaer, U. Griebner, and T. Elsaesser, Opt. Lett. **41**, 4668 (2016).
8. K. Murari, H. Cankaya, P. Kroetz, G. Cirmi, P. Li, A. Ruehl, I. Hartl, and F. X. Kärtner, Opt. Lett. **41**, 1114 (2016).
9. P. Kroetz, G. Chatterjee, A. Ruehl, K. Murari, F. X. Kärtner, I. Hartl, and R. J. D. Miller, *Conference on Lasers and Electro-Optics* (OSA, 2016), p. SF2I.2.
10. F. Bergmann, M. Siebold, M. Loeser, F. Röser, D. Albach, and U. Schramm, Appl. Sci. **5**, 761 (2015).
11. M. Hinkelmann, D. Wandt, U. Morgner, J. Neumann, and D. Kracht, Opt. Express **26**, 18125 (2018).
12. M. Hinkelmann, D. Wandt, U. Morgner, J. Neumann, and D. Kracht, Opt. Express **25**, 20522 (2017).
13. B. M. Walsh, N. B. Barnes, and B. D. Bartolo, J. Appl. Phys. **83**, 2772 (1998).
14. L. von Grafenstein, M. Bock, G. Steinmeyer, U. Griebner, and T. Elsaesser, Laser Photonics Rev. **10**, 123 (2016).
15. P. Kroetz, A. Ruehl, K. Murari, H. Cankaya, F. X. Kärtner, I. Hartl, and R. J. D. Miller, Opt. Express **24**, 9905 (2016).
16. D. Du, X. Liu, G. Korn, J. Squier, and G. Mourou, Appl. Phys. Lett. **64**, 3071 (1994).
17. D. Milam, M. J. Weber, and A. J. Glass, Appl. Phys. Lett. **31**, 822 (1977).
18. R. Adair, L. L. Chase, and S. A. Payne, Phys. Rev. B **39**, 3337 (1989).